Int. J. Electrochem. Sci., 9 **(2014)** 4000 - 4013

International Journal of
ELECTROCHEMICAL
SCIENCE
www.electrochemsci.org

Effect of Current Density on the Corrosion Protection of Poly(o-toluidine)-coated Stainless Steel

Aisha Ganash

Chemistry Department, Faculty of Science, King Abdulaziz University, Jeddah, Saudi Arabia
E-mail: aganash@kau.edu.sa

Received: 21 February 2014 / *Accepted:* 11 March 2014 / *Published:* 14 April 2014

This study examines the use of poly(o-toluidine) (POT) coatings for the corrosion protection of type-304 austenitic stainless steel (SS) in natural seawater. The POT coating was synthesized on the SS substrates from an aqueous solution of H2SO4under galvanostatic conditions using various current densities. The resulting POT coating was uniform, shiny and strongly adherent to the steel substrates. The polymer coating was characterized by UV-visible absorption spectroscopy, Fourier transform infrared (FTIR) spectroscopy, and scanning electron microscopy (SEM). The ability of POT to serve as a corrosion-protective coating for stainless steel was examined by measuring the change in the open-circuit potential (E_{ocp}) overtime, the potentiodynamic polarization, and the results of electrochemical impedance spectroscopy (EIS). The results of this study clearly show that the POT prepared with the lowest current density provides the best protection against corrosion in a natural seawater environment.

Keywords: Galvanostatic; SEM; EIS; Polarization; conducting polymer.

1. INTRODUCTION

Stainless steel belongs to the category of metals that protect themselves against corrosion by forming an oxide (passive) film, which naturally develops on the metal surface under normal atmospheric conditions. The oxide film formed on the steel surface is non-uniform, thin and non-coherent. Therefore, it provides a certain level of protection under normal conditions. When exposed to environments containing halide ions (e.g., seawater), of which the chloride (Cl^-) ion is the most frequently encountered, the oxide film breaks down at specific points, leading to the formation of pits on the metal surface; this type of corrosion is known as pitting corrosion[1–4]. In general, the pitting potential decreases and the corrosion rate increases markedly with increasing chloride concentration. There exist several studies on the pitting corrosion of stainless steels in artificial or natural seawater[5–

7]. Polystyrene layers have been coated ontotype-304 stainless steel and have produced an effective barrier against corrosion and adhesion of corrosion-relevant microorganisms in artificial seawater[8].Three different types of stainless steel,304, 316, and 630, were studied in seawater and the pitting potentials of the type-304, 316, and 630 stainless steels were 0.300, 0.323, and 0.260 V, respectively[9]. Yashiro, et al. [10]reported that the pitting potential of type-304 stainless steel shifts negatively and linearly with the logarithm of the Cl^- concentration in diluted seawater solutions. El-Dahshan et al. studied the corrosion behavior of type-316 stainless steel in Arabian Gulf water[11].Al-fozan et al. found the depth of pitting in 304SS more than in 316SS[12].

Corrosion is an undesirable natural process that arises in the use of metallic materials; therefore, serious efforts to prevent this phenomenon have been ongoing throughout this century. Three approaches are commonly applied to reduce the rate of corrosion, including cathodic protection, anodic protection (passivation) and application of barrier coatings[13]. Various types of polymers have been used as barrier coatings to prevent metals from corroding.

Electrically conducting polymers are the subject of continuous research and development for potential applications in optical and electronic devices[14], electromagnetic shielding[15],energy storage systems[16], corrosion protection[17], sensors[18]and microelectronic devices[19].

A successful electropolymerization on an active metal generally requires a passive layer to prevent the dissolution of the metal and at the same time to oxidize monomers into polymers. Sometimes, a primer polymer coating has also been required to ensure a firm binding deposit onto the base metal. Polyaniline and polypyrrole and their derivatives have been widely investigated because of the low potential for polymer formation and the easy preparation and stability of the formed films. It was demonstrated that ring-substituted conducting polymers[20],such as poly(o-anisidine), poly(o-toluidine), poly(m-toluidine)and poly(o-chloroaniline), can improve the corrosion performance in aggressive environments as do straight-chain polymers, such as PANI and PPy.

A series of studies have reported that polymer films based on thiophene[21], o-phenylenediamine[22], N-methyl pyrrole[23],2,5-dimethoxyaniline[24] and other heterocyclic compounds reduce the corrosion rate of steel and iron in sulfuric acid and chloride solutions.

Aqueous electrochemical polymerization has been preferred to give primer-base coatings on metals because of obvious advantages. Electroactive polymer coatings have emerged as successful alternatives to the harmful chromium-based corrosion inhibitors in combating corrosion[25–32].

Polymers obtained from substituted anilines show properties that differ somewhat from those of PANI. For instance, o-anisidine is a substituted derivative of aniline with a methoxy (OCH_3) group substituted at the ortho position. A review presented the use of poly(o-anisidine) for corrosion control, focusing on structural alloys for the aerospace industry, such as Al 2024[33], mild steel[34], platinum[35] and copper[36].Poly(o-toluidine)(POT), the polymer derived from o-toluidine (OT)(substituted aniline with a $–CH_3$ group on the aromatic ring in the ortho position),has been reported to show structural properties and redox and electro chromic behavior closely related to those of PANI[37–41].

POT with hydrophobic groups may be able to lower the water-up take rate, or another group may enhance its stability and adherence. Just like PANI, POT also exists in various oxidation states. It shows an insulator-to-conductor transition from its reduced leucoemeraldine to emeraldine state upon

oxidation. The electrical conductivity of conducting materials is a crucial factor in addition to their electroactivity in potential applications. Interest in the understanding of electronic conductivity and the correlation between the electrochemical and spectroelectro chemical properties of conjugated polymers increases rapidly[42].

A number of studies have found that poly(o-toluidine)(POT) acts as a protective coating on active metals such as steel materials[43–46]. The anticorrosive properties of poly(o-toluidine) and its copolymer with polyaniline and polypyrrole on mild steel were investigated in artificial seawater[47, 48]. Shinde et al. synthesized POT on a copper substrate using cyclic voltammetry from an aqueous solution of sodium oxalate. The resulting POT coating was uniform and strongly adherent to the Cu substrate. They examined the use of poly(o-toluidine) (POT) coatings for the corrosion protection of copper (Cu) in an aqueous solution on platinum substrates of 3% NaCl[49].Poly(o-aniline-co-o-toluidine) (PA-co-POT) films were synthesized by changing the mole ratio of the monomers, and they were characterized by cyclic voltammetry, UV-visible and FTIR spectroscopy, and thermo gravimetric analysis (TGA)[50].The chemically oxidative copolymerization of pyrrole with m-toluidine copolymers and poly(o-m-toluidine-co-o-nitroaniline) has also been reported[51, 52].

This paper attempts to (1) show the effect of various current densities on the electrodeposition of poly(o-toluidine) coatings by the galvanostatic method on type-304 stainless steel (SS) substrates from an aqueous solution containing o-toluidine and sulfuric acid and(2) explore its corrosion protection behavior by measuring the change in the open-circuit potential (E_{opc}) with time, polarization and EIS techniques in natural seawater.

2. EXPERIMENTAL METHODS

To assess the effect of seawater pitting corrosion behavior on SS materials,type-304 austenitic SS was tested in natural seawater at room temperature (25 °C).The chemical analyses (in wt. %) of 304SS are listed in Table 1.

In all of the electrosynthesis experiments, an aqueous solution containing 0.2 M of the monomer and 0.5 M of H_2SO_4 acid was prepared by using doubly distilled water. Electropolymerization and corrosion tests were performed in a conventional three-electrode system using 304SS as the working electrode, a platinum sheet as the counter electrode and Ag/AgCl (3 mol dm^{-3}KCl) as the reference electrode. The working electrode was constructed from a304SS rod with a 6-mm diameter. Experiments were performed at 25 °C in stagnant natural seawater. The chemical composition of the seawater used during this study is given in Table 2.

The steel surface was polished using emery paper of successive grades up to 1500. The steel electrode was washed thoroughly with redistilled water and acetone in an ultrasonic bath before immersion into the electrolytic solution. POT was electrochemically synthesized from an aqueous acidic solution containing the monomer by keeping a fixed current for a fixed duration of time. Four current densities, 5, 10, 15 and 20 mA cm^{-2}, were attempted, and the corresponding potential transients were recorded for a period of 1800 s.

The corrosion protection of the polymer coatings was studied with measurements of the open-circuit potential (E_{ocp}), the Tafel test and electrochemical impedance spectroscopy (EIS) in natural seawater at room temperature.

The Tafel tests were conducted in natural seawater (scan range of -0.200 to +0.200 V)vs. E_{ocp} at a scan rate of 1 mV s^{-1}.All impedance measurements were recorded at open-circuit potentials in the frequency range of $5x10^4$ to 0.01 Hz using an AC amplitude of 10 mV. The electrochemical experiments were performed using an Autolab PGSTAT30 potentiostat coupled with a computer equipped with GPES software for potential and FRA for EIS. Fourier transforms infrared (FTIR) spectra of the polymer films were measured using a Perkin-Elmer FTIR spectrometer. Scanning electron microscopy (SEM) data were obtained using a JEOL JSM-6360LVSEM.

The optical absorption study of these films was performed using a Varian Cary 50 Conc UV/Vis spectrophotometer. The UV-visible spectra were obtained in DMSO. All of the spectra were recorded in the wavelength range of 200–1100 nm.

Table 1. Chemical composition (wt. %) of 304 stainless steel samples

Element	C	Mn	Si	S	P	Ni	Cr	Mo	Cu	N	Co
wt. %	0.03	1.45	0.43	0.02	0.041	8.08	18.23	0.34	0.50	0.82	0.13

Table 2. Chemical composition of seawater

Constituents	Amount
Cations (ppm)	
Sodium	11,368
Potassium	348
Calcium	541
Magnesium	1224
Anions (ppm)	
Chloride	52,390
Sulfate	6169
Fluoride	58.9
Other parameters	
Conductivity (mS/cm)	54.20±0.081
pH	7.707±0.021
Dissolved oxygen (ppm)	7.74±0.069
Total dissolved solids (ppm)	54,15±0.057

3. RESULTS AND DISCUSSION

3.1. Galvanostatic synthesis

Fig. 1 shows the E-t curves, which were obtained during the formation of the POT coatings on 304SS for four different constant current densities, 5, 10, 15 and 20 $mAcm^{-2}$,for 1800 s. At the end of

each experiment, a greenish-black homogeneous coating was observed. The thickness of the POT electrodeposited on the SS was measured experimentally and found to be approximately 0.93 mm.

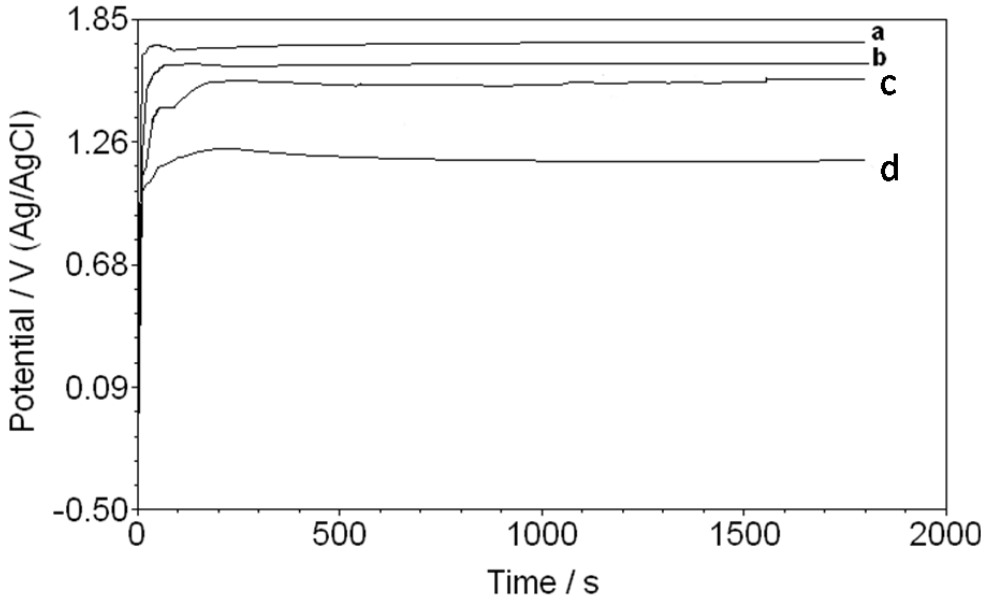

Figure 1. Galvanostatic polymerization in 0.5 M H_2SO_4 acid solution containing 0.2 M o-toluidine at current densities a)**20**, b)1**5**, c)1**0** and d)**5** mA cm^{-2}.

3.2. Spectroscopic characterization

FTIR spectra were used to characterize the structure of the POT coating prepared by 5 $mAcm^{-2}$ after peeling it off the metal surface, and they are presented in Fig.2.

For POT, the absorption band at approximately 3219 cm^{-1} corresponds to the N–H stretching mode of a secondary amine. The two bands at approximately 1589 and 1531 cm^{-1} are assigned to the stretching vibration of the benzenoid-quinoid ring. The characteristic bands at approximately 2828 cm^{-1} can be assigned to the stretching vibration of the methyl ($–CH_3$) group. The bands at 1488 cm^{-1} are due to the symmetric deformation of the methyl group. The bands at 1146cm^{-1} can be assigned to the C–N vibration. The three bands appearing at 804, 753 and 1100cm^{-1} were attributed to an out-of-plane C–H vibration, a 1,2,4-substitution in the benzenoid rings, and an in-plane C–H vibration of quinoid rings, respectively.

Fig.3 shows the optical absorption spectrum of the poly(*o*-toluidine) doped with H_2SO_4 acid, recorded using *DMSO* as the solvent. The spectrum reveals the presence of a sharp peak at 320 nm with a shoulder at 420 nm and a broad peak at approximately 500 - 800 nm. The peak at 320 nm corresponds to the π-π^* transition of the benzenoid rings, whereas the shoulder at 420 nm can be assigned to the localized polarons that are characteristic of the protonated polymer backbone. The emeraldine salt phase of the polymer, the only electrically conducting phase of POT, appears at

approximately 700 nm, where as the peaks at 540 - 640 nm represent the insulating pernigraniline phase of the polymer[53].

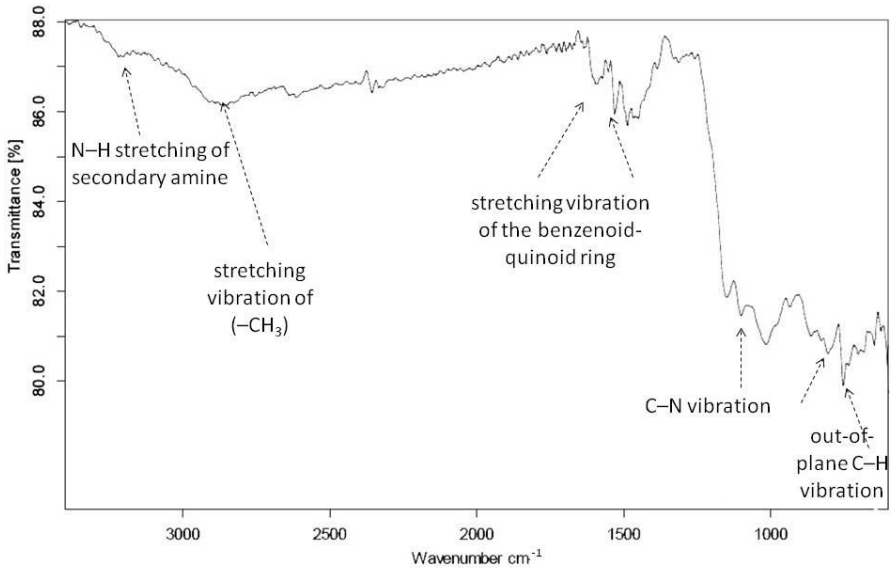

Figure 2. FTIR spectra (4000-500 cm^{-1}) of POT film.

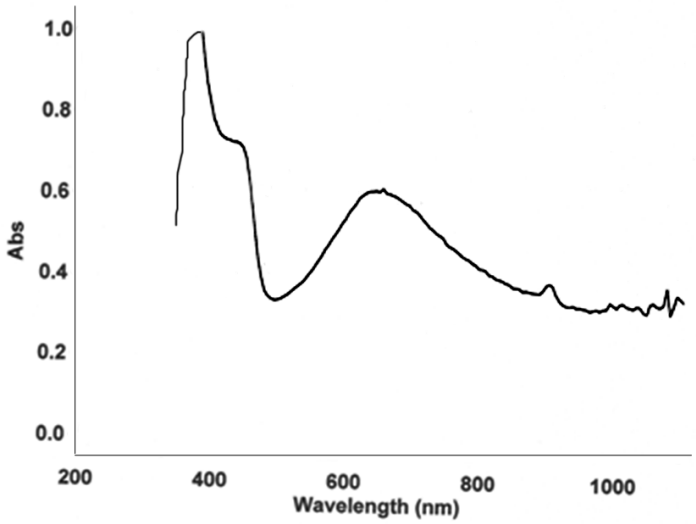

Figure 3. UV spectra (200-1100 nm) of POT film.

3.3. Morphological characterization

The effects of the pulse amplitude (current density) on the morphology and the size of the particles of the synthesized POT were investigated.Fig.4 shows typical SEM images of POT-coated SS under various densities. The porosity of the low current density (5 mA cm^{-2}) sample was less than that of samples prepared at other current densities. A comparison of the images shows that POT becomes more porous with a higher current density, which facilitated the access of the corrosive chloride ions to the metal surface.

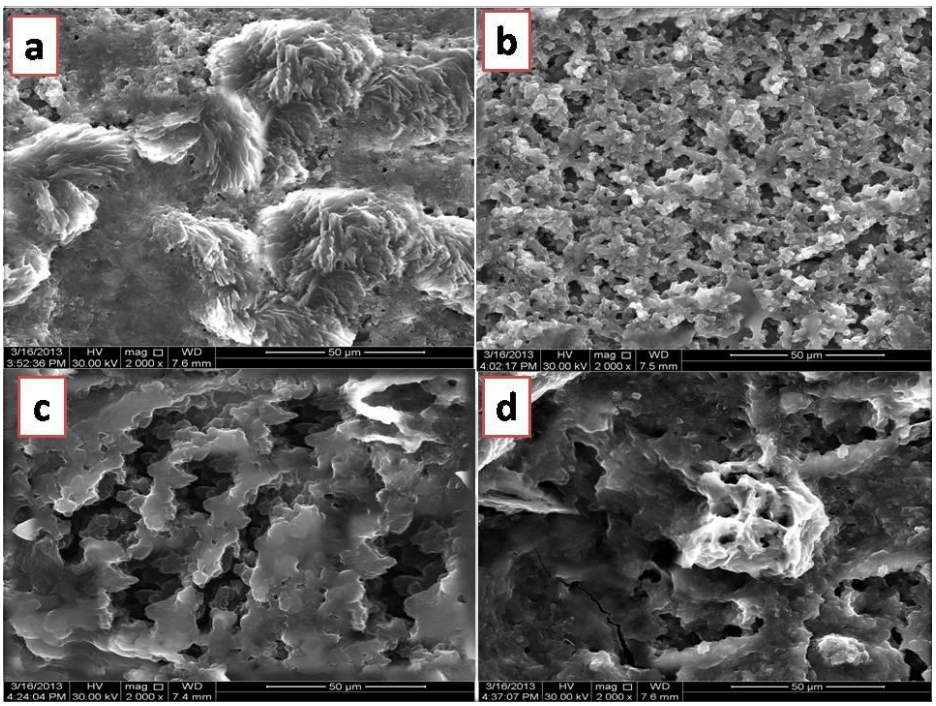

Figure 4. SEM images of POT coated 304 SS at current densities a)5, b)10, c)15 ,d)20 mA cm^{-2}

3.4. Effect of the various current densities on the protection of SS

The polymer-coated sample, as well as a bare (uncoated) stainless steel sample, was immersed into seawater at 25 °C, and the potential of the steel was monitored with time, as shown in Fig.5. E_{ocp}-time curves are generally used to understand the efficiency of the conducting polymer during corrosion tests because the kinetics of the reduction reactions of O_2 and H_2O depends on the E_{ocp} value of the bare metal. When a metal is coated with a highly doped conducting polymer, as long as the conducting polymer remains in its conductive state, the E_{ocp} value of the conducting polymer/metal system is always larger than that of the bare metal electrode. When the conducting polymer is reduced, the potential value drops to a lower value[54]. The open-circuit potential (OCP) of uncoated stainless steel was initially the negative value of -0.200 V and remained in the active state at the end of the experiment. In contrast, the coated samples had positive open-circuit potentials from the beginning of the measurement. However, the open circuit potential decreased with the passage of time and finally reached the value of -0.025 V (Ag/AgCl) for 20 $mAcm^{-2}$, which indicates that the polymers were able to passivate the steel surface. Oscillations of the potential can be observed. These oscillations are associated with the attacking chloride ions causing a pitting in the electrode surface. This case was simply related to the physical barrier behavior of the polymer coating between the corrosive environment and the underlying metal. In the case of the coated samples, corrosion could occur within the pores of the polymer film, where the corrosive solution could access the polymer layer and reach the metal surface.

The adherence of the electrosynthesized coatings to the substrate was evaluated after immersion in seawater. The adherence of the POT films electrosynthesized at various current densities

was tested using adhesive tape. It was found that the adhesion was strong and the coating could only be removed by polishing.

However, these pits are not sustained, which can be checked by removing the film; the surface remains smooth overall with slightly depressed areas.

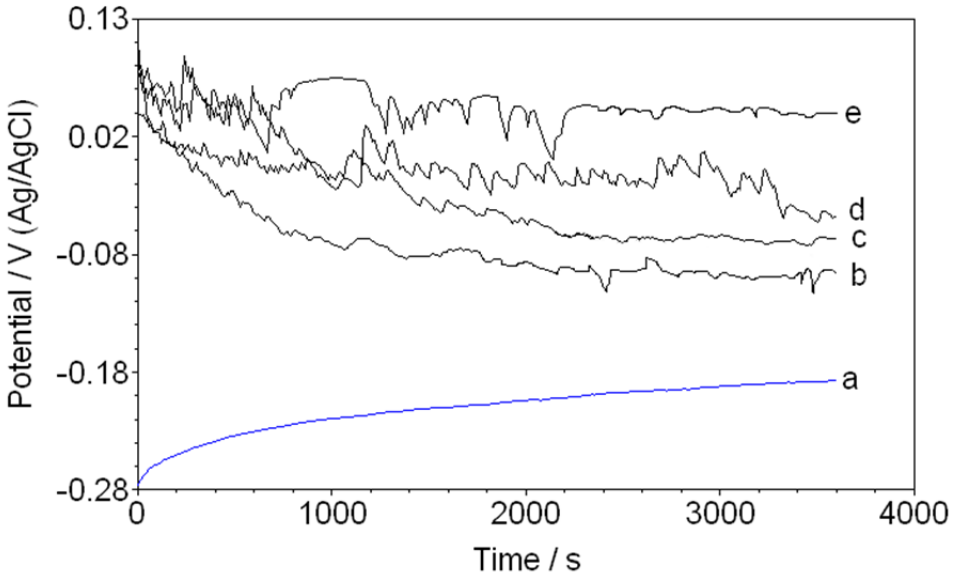

Figure 5. Potential-time behaviour of a) uncoated and POT coated 304 SS at current densities b)20, c)15, d)10 and e)5 mA cm^{-2} in seawater.

The electrochemical Tafel slope analysis was performed to evaluate the anticorrosion performance of the POT coatings prepared at various current densities as well as the uncoated 304SS samples.

The Tafel plots for various uncoated and coated samples were recorded by sweeping the potential from the equilibrium potential toward negative and positive potentials against an Ag/AgCl reference electrode. Fig.6 shows the Tafel plots of POT-coated stainless steel for the various current densities in seawater. The corrosion potential (E_{corr}),the corrosion current density I_{corr} derived by extrapolating the anodic and cathodic Tafel lines at E_{corr}, the polarization resistance (R_p), the anodic and cathodic Tafel slopes (β_a and β_c) and the corrosion rate (CR)are obtained from the GPES software and tabulated in Table 3; generally, a higher E_{corr} and a lower I_{corr}, R_p and CR indicate better corrosion protection.

The figure shows that the corrosion potential value (**E_{corr}**) for the uncoated SS sample was negative and the corrosion potentials of the POT-coated stainless steel are nobler in comparison with bar stainless steel; this indicates that the passivating tendency of the POT coating due to its behavior as a physical barrier between the corrosive environment and the metal substrate. In addition, as shown in Table 3, the anodic Tafel slopes and the cathodic Tafel slopes are not significantly affected by the change the current density, which indicates that the mechanism is independent of the current density.

The corrosion current densities of the coated samples are significantly different than that of the blank. The I_{corr} value decreases from 0.087μAcm^{-2} for uncoated SS to 0.012μAcm^{-2} for POT-coated

SS under the optimal conditions. Additionally, the corrosion rate of SS is significantly reduced as a result of the reduction in I_{corr}. The applied current density of 5 $mAcm^{-2}$ provides the best protection against corrosion in natural seawater, i.e., the minimum corrosion rate and corrosion current values were obtained when the applied current density was a low value in the electrodeposition process. Yalçınkaya et al. have reported that dissolution only occurred along the open pores, and thus, the rate of this process was strictly related to the porosity of coating[55]. Ghoreishi et al. found that poly o-ansinidine formed from 20 $mAcm^{-2}$on an aluminum alloy provided better protection in a 3.5% NaCl solution[56].

The coating porosity is an important parameter that strongly governs the anticorrosive behavior of the coatings. The porosity of the POT coatings on the SS substrates was determined from Tafel measurements. The porosity of the POT coating was calculated using the relation[57]:

$$P = \frac{R_{puc}}{R_{pc}} 10^{-\left(\frac{\Delta E}{ba}\right)},$$

where P is the total porosity, R_{puc} is the polarization resistance of the uncoated SS, R_{pc} is the measured polarization resistance of coated SS, ΔE_{corr} is the difference between the corrosion potentials and ba is the anodic Tafel slope for the uncoated SS substrate. The calculated porosity value of the POT coatings is also given in Table 3. As seen in the table, the porosity value of the coating increases with an increase in the applied current density. To find a probable reason, the electrochemical reactions of aniline electropolymerization can be useful. The mechanism of aniline polymerization reactions has been studied by a number of researchers. The oxidative polymerization of aniline has been shown to proceed via the formation of dimer molecules during the nucleation process, followed by an oligomerization reaction[58–60]. Based on the previously reported reactions, the anilinium cation radical is the main initiator of electropolymerization. Therefore, the production rate of these radicals is the most important factor in controlling the morphology of the product and the size of its particles. At high current densities, the production rate of anilinium cation radicals as the initiator of aniline polymerization is higher than that at low current densities, for which the synthesized polymer does not have a specific and uniform morphology.

Impedance measurements of a stainless-steel electrode and a coated polymer electrode in seawater vs. an Ag/AgCl reference electrode were performed at a corrosion potential in the frequency range from $5x10^4$ to 10^{-1} Hz, with a value of 10 mV for the amplitude.

Table 3. Polarisation parameters for POT-coated SS in natural seawater.

sample	E_{corr} /V	$j_{corrosion}$ /A cm^{-2}	ba(V dec^{-1})	bc(V dec^{-1})	Rp /Ohm cm^2	Corrosion rate/mm $year^{-1}$	Porosity(%)
Uncoated SS	-0.200	8.70 X 10^{-8}	0.298	0.079	3.65 X 10^3	1.91 X 10^{-3}	------
20 mA cm^{-2}	-0.131	6.70 X 10^{-8}	0.099	0.088	1.03 X 10^4	1.55 X 10^{-3}	4.64
15 mA cm^{-2}	-0.086	6.06 X 10^{-8}	0.074	0.104	1.45 X 10^4	1.41 X 10^{-3}	2.84
10 mA cm^{-2}	-0.065	4.13 X 10^{-8}	0.074	0.093	2.40 X 10^4	9.57 X 10^{-4}	1.59
5 mA cm^{-2}	-0.025	1.25 X 10^{-8}	0.092	0.104	3.61 X 10^4	7.14 X 10^{-4}	0.93

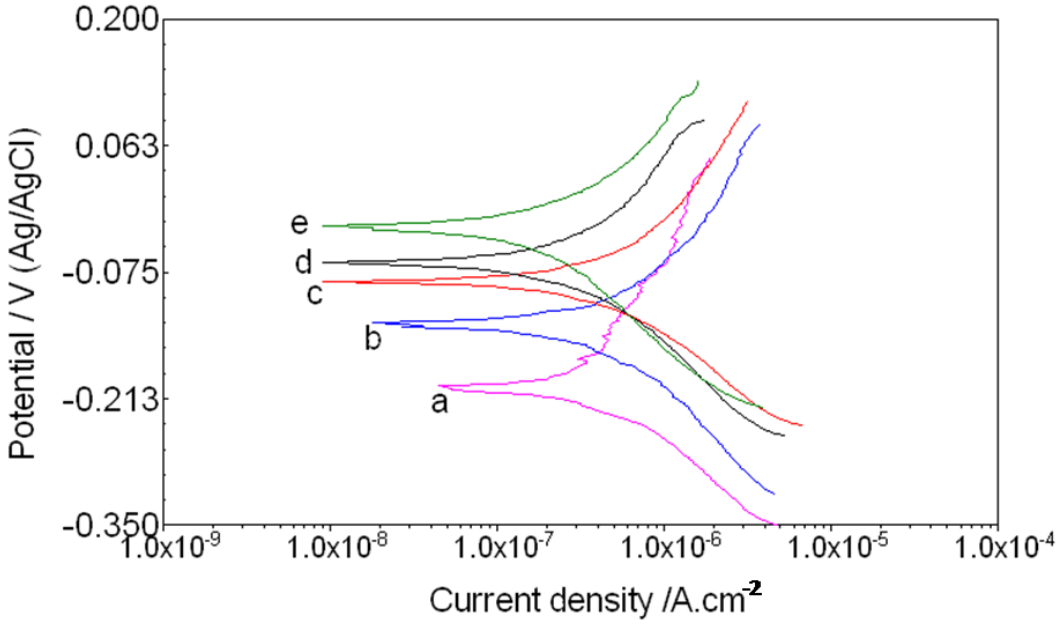

Figure 6. Polarization behavior of a) uncoated and POT coated 304 SS at current densities b)20, c)15, d)10 and e)5 mA cm^{-2} in seawater.

Fig. 7 shows the impedance spectrum of uncoated steel obtained in seawater. The Nyquist plots were recorded at the corrosion potential after an exposure time of one hour in neutral seawater. Fig. 7shows that the impedance plots obtained for POT-coated SS at various current densities in seawater are different than that of the uncoated SS electrode. In the case of uncoated steel, it is important to note that there was not any coating on the steel surface, and therefore, passivation of the steel surface cannot be expected. Hence, the diameter of the impedance plot must be equal to the charge transfer resistance value of the stainless steel[61]. The equivalent circuit depicted in Fig. 8 (a) modeled this impedance plot. The equivalent circuit consists of the electrolyte resistance (R_s), the charge-transfer resistance (R_{ct}) and the constant phase element (CPE) Q_{dl}.

The impedance plots of the POT coatings at various current densities are consistent, featuring a semicircle in the high-frequency region. This impedance arc is attributable to the process occurring at the polymer-electrolyte interface, which is expected to be the double-layer capacitance in parallel with the ionic charge-transfer resistance, due to the ion exchange for charge compensation at the polymer-solution interface[62].The impedance responses rise to attain a vertical line in the low-frequency region. This deviation from the ideal vertical line is most likely due to the irregular geometry of the polymer surface. This impedance plot was modeled by the equivalent circuit shown in (Fig. 8(b)) to clarify the corrosion protective properties of polymer films electropolymerized on SS electrodes. The model assumes that the reduction process of the coating promotes the oxidation of the substrate. R_s represents the solution resistance, R_p is the pore resistance and R_{ct} is the charge-transfer resistance of the area at the metal/coating interface at which corrosion occurs and is connected with the corrosion processes in the bottom of the pores.CPE is associated with the non-ideal double-layer capacitance of the POT/solution interface. Q_c represents the constant phase element due to the capacity of the polymer coating. The results of the fitting are presented in Table 4. CPE is symbolized as Q in the equivalent

circuit. The physical meaning of CPE has been discussed by many authors and is related to surface heterogeneity[63].The higher values of R_{ct} and R_{por} and the lower values of C_c and C_{dl} indicate the excellent corrosion performance of the polymer coating. As seen in Table 4, the value of R_{ct} is higher for lower applied current densities, which is attributed to an increase the effective barrier behavior of the polymer coating. Higher R_{ct} values were evidence of the formation of a stable, passive layer at the polymer/electrode interface. In other words, the corrosive constituents are restricted to diffuse metal because of the polymer coating. Comparatively, as the applied current density increased, the polymer film resistance decreased, and the coating capacitance increased. The increase in the capacitance values is an indication of the increase of electrolyte uptake[64].

Several mechanisms have been suggested during recent years that basically consider a conducting polymer either as a barrier coating alone or as an active coating participating to the reactions taking place across the polymer-coated metal and electrolyte interface[20, 65].A metal substrate coated with a charged conducting polymer will place the electrode potential in the passive range in the absence of any redox reaction. However, in the presence of a redox reaction, which is inevitable even in the passive regime, the conducting polymer film will discharge. Consequently, the potential will drift toward negative values. The length of time during which the potential is maintained in the passive regime depends on the total charge stored in the polymer and the rate of the reaction. Therefore, for sustained protection, the polymer film must be charged continuously. This is done by cathodic reduction of oxygen on the polymer[66]:

$$M \rightarrow M^{n+} + ne^{-}. \quad (1)$$

The generated electron discharges the polymer:

$$poly^{n+} + ne^{-} \rightarrow poly^{0}. \quad (2)$$

The polymer is recharged by reduction of oxygen on the polymer surface:

$$poly^{0} + \frac{n}{4}O_2 + nH^{+} \rightarrow poly^{n+} + \frac{n}{2}H_2O. \quad (3)$$

Therefore, the overall reaction (1+2+3) is:

$$M + \frac{n}{4}O_2 + nH^{+} \rightarrow \frac{n}{2}H_2O + M^{n+}. \quad (4)$$

The theory clearly shows the importance of the oxygen reduction reaction of the polymer surface.

Table 4. Impedance parameters for POT- coated SS in natural seawater.

sample	Rs/Ω cm^2	Rp/kΩ cm^2	Rct/kΩ cm^2	Qc		Qdl	
				Cc(F cm^{-2})	n_1	Cdl(F cm^{-2})	n_2
20 mA cm^{-2}	2.82	2.02	2.30	0.36 x10^{-03}	0.85	0.53 x10^{-06}	1.00
15 mA cm^{-2}	0.34	5.37	5.46	0.20 x10^{-03}	0.89	0.10 x10^{-06}	0.99
10 mA cm^{-2}	0.89	6.73	9.41	0.19 x10^{-03}	0.85	0.14 x10^{-06}	0.99
5 mA cm^{-2}	1.42	9.57	15.14	0.11 x10^{-03}	0.96	0.32 x10^{-04}	0.48

The experimental results of the present study reveal that a higher current density of 20 $mAcm^{-2}$affects the morphology of the polymer and increases the porosity of the layer, which facilitates the passage of aggressive chloride ions to reach the metal surface and begin pitting corrosion; in contrast, the POT coating formed from a current density of 5 $mAcm^{-2}$was less porous and exhibits better corrosion protection properties compared to POT produced by the other current densities.

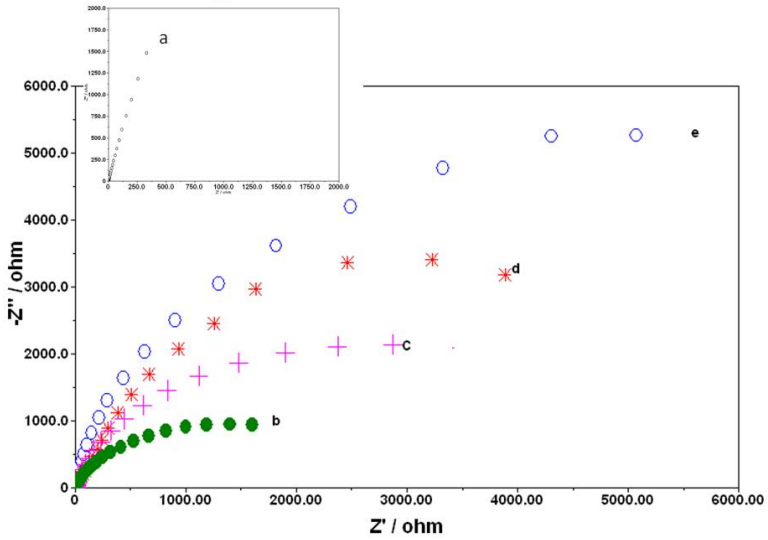

Figure 7. Nyquist impedance plots of a) uncoated and POT coated 304 SS at current densities b)20, c)15, d)10 and e)5 mA cm^{-2} in seawater.

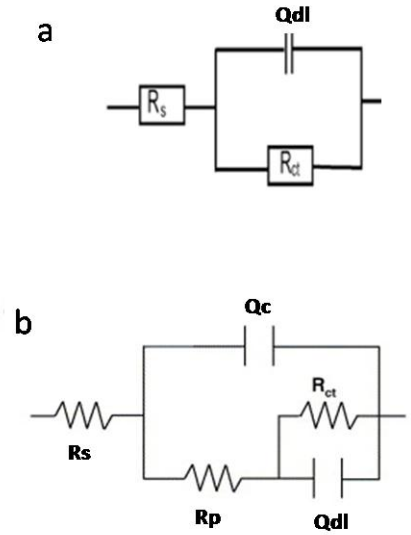

Figure 8. Equivalent circuits representing the impedance behaviour of a) uncoated and b) coated electrodes.

4. CONCLUSIONS

Homogeneous and adherent POT coatings were successfully synthesized on SS using a galvanostatic technique with various current densities (5, 10, 15 and 20 $mAcm^{-2}$) for 1800 s from an

aqueous solution containing o-toluidine and H_2SO_4. The Tafel polarization and EIS studies reveal that the POT acts as a protective layer on the SS against corrosion in seawater. The porosity in the coating was evaluated using Tafel polarization measurements, and it was observed that the porosity depends on the applied current density. The POT coating synthesized using a current density of $5mAcm^{-2}$is more compact and provided more corrosion protection in natural seawater than the other applied current densities.

References

1. R. L. Horst, *Materials Performance* 16(1977) 23.
2. P. M. Natishan, E. McCafferty, and G. K. Hubler, 86(1986) 437.
3. B. A. Shaw, G. D. Davis, T. L. Fritz, B. J. Rees, and W. C. Moshier, *Journal of the Electrochemical Society* 138(1991) 3288.
4. Z. Szklarska-Smialowska, *Corrosion Science* 41(1999) 1743.
5. S. S. Xin and M. C. Li, *Corrosion Science,*81(2014) 96
6. S. Yuan, B. Liang, Y. Zhao, and S. O. Pehkonen, *Corrosion Science* 74(2013) 353.
7. A. Toro, A. Sinatora, D. K. Tanaka, and A. P. Tschiptschin, *Wear* 251(2001) 1257.
8. L. Románszki, I. Datsenko, Z. May, J. Telegdi, L. Nyikos, and W. Sand, Bioelectrochemistry .doi:10.1016/j.bioelechem.2013.10.002
9. S.-K. Jang, M.-S. Han, and S.-J. Kim, *Transactions of Nonferrous Metals Society of China* 19(2009) 930.
10. H. Yashiro, K. Tanno, S. Koshiyama, and K. Akashi, *Corrosion* (Houston) 52(1996) 109.
11. M. E. El-Dahshan, A. M. Shams El Din, and H. H. Haggag, *Desalination* 142(2002) 161.
12. S. A. Al-Fozan and A. U. Malik, *Desalination* 228(2008) 61.
13. A. Olad and B. Naseri, *Progress in Organic Coatings* 67(2010) 233.
14. H. He, J. Zhu, N. J. Tao, L. A. Nagahara, I. Amlani, and R. Tsui, *J. Am. Chem. Soc.* 123(2001) 7730.
15. W.-K. Lu, R. L. Elsenbaumer, and B. Wessling, *Synthetic Metals* 71(1995) 2163.
16. J.-M. Pernaut and J. R. Reynolds, *J. Phys. Chem*. B 104(2000) 4080.
17. J.-M. Yeh and K.-C. Chang, *J. Ind. Eng. Chem*. 14(2008) 275.
18. G. Inzelt, M. Pineri, J. . Schultze, and M. . Vorotyntsev, *Electrochimica Acta* 45(2000) 2403.
19. B. Wessling, P. K. Kahol, A. Raghunathan, and B. J. McCormick, *Synthetic Metals* 119(2001) 197.
20. D. Sazou, *Synthetic Metals* 118(2001) 133.
21. U. Rammelt, P. . Nguyen, and W. Plieth, *Electrochimica Acta* 46(2001) 4251.
22. S. S. Abd El Rehim, S. M. Sayyah, M. M. El-Deeb, S. M. Kamal, and R. E. Azooz, *Materials Chemistry and Physics* 123(2010) 20.
23. T. Tüken, G. Tansuğ, B. Yazıcı, and M. Erbil, *Surface and Coatings Technology* 202(2007) 146.
24. Patil V., Sainkar S.R., and Patil P.P., *Synthetic Metals* 140(2004) 57.
25. K. Kamaraj, S. Sathiyanarayanan, and G. Venkatachari, *Progress in Organic Coatings* 64(2009) 67.
26. P. Ocón, a. B. Cristobal, P. Herrasti, and E. Fatas, *Corrosion Science* 47(2005) 649.
27. H. R. Garner, (1982).at http://adsabs.harvard.edu/abs/1982PhDT. 9G.
28. K. M. Cheung, D. Bloor, and G. C. Stevens, *Polymer* 29(1988) 1709.
29. S. Saidman, *Journal of Electroanalytical Chemistry* 534(2002) 39.
30. K. Naoi, Y. Oura, A. Yoshizawa, M. Takeda, and M. Ue, *Electrochemical and solid-state letters* 1(1998)34.
31. K. Naoi, M. Takeda, H. Kanno, M. Sakakura, and A. Shimada, *Electrochimica Acta* 45(2000)

3413.
32. K. Shah and J. O. Iroh, *Surface Engineering* 20(2004) 53.
33. K. Shah and J. Iroh, *Advances in Polymer Technology* 23(2004) 291.
34. S. Chaudhari and P. P. Patil, *Journal of Applied Polymer Science* 106(2007) 400.
35. A. T. Ozyilmaz, G. Ozyilmaz, and O. Yigitoglu, *Progress in Organic Coatings* 67(2010) 28.
36. S. Chaudhari, S. R. Sainkar, and P. P. Patil, *J. Phys. D: Appl. Phys*. 40(2007) 520.
37. S. Cattarin, L. Doubova, G. Mengoli, and G. Zotti, *Electrochimica Acta* 33(1988) 1077.
38. R. J. Mortimer, *J. Mater. Chem*. 5(1995) 969.
39. M. Leclerc, J. Guay, and L. H. Dao, *Macromolecules* 22, 649 (1989).
40. M. Probst and R. Holze, *Macromolecular Chemistry and Physics* 198(1997) 1499.
41. M. Probst and R. Holze, Berichte der Bunsengesellschaft für physikalische Chemie 100(1996) 1286.
42. S. Bilal, A.-H. A. Shah, and R. Holze, *Electrochimica Acta* 54(2009) 4851.
43. V. Shinde and P. P. Patil, *Materials Science and Technology* 19(2003) 1603.
44. V. P. Shinde and P. P. Patil, *J Solid State Electrochem* 17(2013) 29.
45. V. Shinde, S. R. Sainkar, and P. P. Patil, *Journal of Applied Polymer Science* 96(2005) 685.
46. V. Shinde, S. Chaudhari, P. Patil, and S. Sainkar, *Materials Chemistry and Physics* 82(2003) 622.
47. M. Mobin and N. Tanveer, *Protection of Metals and Physical Chemistry of Surfaces* 48(2012) 243.
48. M. Mobin and N. Tanveer, *Journal of Coatings Technology & Research* 9(2012) 27.
49. V. Shinde, S. R. Sainkar, and P. P. Patil, *Corrosion Science* 47(2005) 1352.
50. D. D. Borole, U. R. Kapadi, P. P. Mahulikar, and D. G. Hundiwale, *Materials Letters* 60(2006) 2447.
51. X.-G. Li, M.-R. Huang, L.-X. Wang, M.-F. Zhu, A. Menner, and J. Springer, Synthetic Metals 123(2001) 435.
52. P. Savitha and D. N. Sathyanarayana, *Synthetic Metals* 145(2004) 113.
53. A. A. Athawale, M. V. Kulkarni, and V. V. Chabukswar, *Materials Chemistry and Physics* 73(2002) 106.
54. P. Camille Lacaze, J. Ghilane, H. Randriamahazaka, and J.-C. Lacroix, Electroactive Conducting Polymers for the Protection of Metals against Corrosion: from Micro- to Nanostructured Films, in Nanostructured Conductive Polymers, Edited by A. Eftekhari, John Wiley & Sons, Ltd (2010), pp. 631–680.at <http://onlinelibrary.wiley.com/doi/10.1002/9780470661338.ch16/summary>
55. S. Yalçınkaya, T. Tüken, B. Yazıcı, and M. Erbil, *Current Applied Physics* 10(2010) 783.
56. S.M.Ghoreishi, M. Shabani-Nooshabadi, M. Behpour, and Y. Jafari, *Progress in Organic Coatings* 74(2012) 502.
57. S. Chaudhari, S. R. Sainkar, and P. P. Patil, *J. Phys. D: Appl. Phys.* 40(2007) 520.
58. 5K. Bade, V. Tsakova, and J. W. Schultze, *Electrochimica Acta* 37(1992) 2255.
59. H. Yang, D. O. Wipf, and A. J. Bard, *Journal of Electroanalytical Chemistry* 331(1992) 913.
60. B. J. Johnson and S.-M. Park, *Journal of the Electrochemical Society* 143(1996) 1277.
61. G. W. Walter, *Corrosion Science* 26(1986) 681.
62. G. Láng and G. Inzelt, *Electrochimica Acta* 44(1999) 2037.
63. F. Fusalba, P. Gouérec, D. Villers, and D. Bélanger, *J. Electrochem. Soc*. 148(2001) A1.
64. M. R. Mahmoudian, W. J. Basirun, Y. Alias, and A. Khorsand Zak, *Thin Solid Films* 520(2011) 258.
65. S. Biallozor and a. Kupniewska, *Synthetic Metals* 155(2005) 443.
66. S. U. Rahman, *Surface and Coatings Technology* 205(2011) 3035.